

pubs.acs.org/Macromolecules Article

Mechanically Tunable and Reconstructable Lignin Thermosets via "Click" Chemistry and Surface Functionalization

Yishayah Bension, Leman Buzoglu Kurnaz, Ting Ge,* and Chuanbing Tang*



Cite This: Macromolecules 2023, 56, 2831-2840



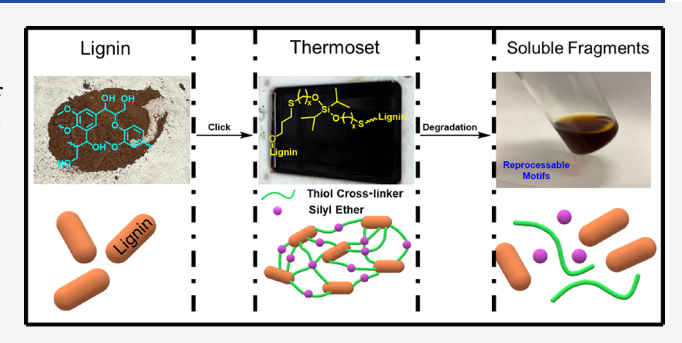
ACCESS I

III Metrics & More

Article Recommendations

Supporting Information

ABSTRACT: Among the most abundant biomass, lignin is an appealing yet challenging feedstock for manufacturing sustainable materials. The polyphenolic structure and globular architecture of lignin makes it a mechanically weak material for being incorporated in polymer composites. Upon surface modification with functionalized silyl ether groups via thiol-ene chemistry in this work, lignin was cross-linked to create reconstructable thermosets. These thermosets exhibit not only enhanced mechanical properties but also improved degradability. The synthesis of different crosslinkers was used to explore the structure-property relationship. Altering the cross-linking density and the size of cross-linkers has a large impact on the mechanical properties of the final thermosets.



Furthermore, the chemical recycling of these thermosets was explored for the conversion to initial motifs under basic environments.

INTRODUCTION

Thermosetting polymers such as epoxy resins and vulcanized rubber offer higher glass-transition temperatures and stronger mechanical properties compared to polymers without crosslinks. 1-3 These materials are formed when polyfunctional groups are covalently cross-linked to create a three-dimensional network. The cross-linking could lead to insoluble rigid materials that are neither degradable nor reprocessable. Since thermosets cannot undergo conventional recycling, they are usually dumped into landfills and waterways, contributing to the global environmental crisis.^{4–6} Therefore, there is a strong need to develop sustainable and recyclable thermosets. One approach is chemical recycling by integrating labile chemical linkages into the network, which can be degraded using specific reaction conditions. For example, incorporating ester bonds into thermosets enables degradability under basic conditions. However, this kind of material is susceptible to hydrolysis at relatively high temperature, which may not be desirable for some high-temperature applications. 8,9 In recent years, reprocessable thermosets have received much attention, most distinctly on developing covalent adaptable networks (CANs) that are sensitive to an external stimulus such as light or heat. 10,11 The degraded fragments of reprocessible thermosets are usually soluble and easily reprocessed.9 In addition to reprocessibility, sustainability of thermosets could be achieved when renewable feedstocks such as biomass are used to design chemically recyclable thermosets. 12

Traditional thermosets are usually derived from petroleum sources with positive carbon emissions. $^{13-15}$ One way to reduce carbon emission and thus increase sustainability is to use renewable feedstocks. To this end, biomass has been

touted as green feedstock toward achieving net-zero carbon emission. Lignin as one of the three major components of wood is a class of representative biomass. 16 Lignin is an irregular amorphous polymer naturally formed by the cross coupling of monolignol radicals. 17,18 Despite its rigidity, raw lignin itself cannot form free-standing films for the measurement of mechanical properties, as their low molecular weights and branched architectures prevent the formation of polymer entanglement, which plays the central role in the mechanical strength of amorphous polymers. Cross-linking lignin to a thermoset provides a viable pathway to enhance the mechanical properties while bypassing the need of polymer entanglement. The current annual production of lignin exceeds 50 million tons, but only a fraction is commercialized for applications such as dispersion agents and surfactants. 19 Given the high abundance and low cost of lignin, there is great interest in valorizing this biomass for sustainable thermosets.

The high hydroxyl content of lignin makes it appealing for undergoing cross-linking reactions. Previous work used different chemistries to cross-link lignin, including epoxide opening, esterification, Diels-Alder, thiol-ene, and many others. Three factors were considered when designing cross-linkers: ease of synthesis, strong bonding, and degrad-

Received: November 30, 2022 Revised: March 16, 2023 Published: March 30, 2023





© 2023 American Chemical Society

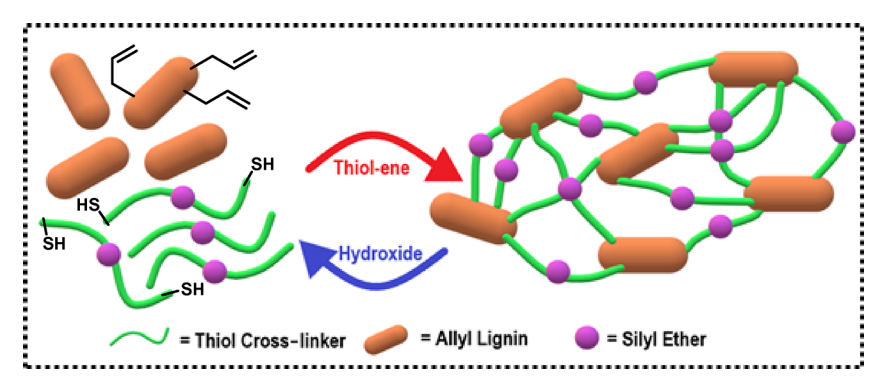


Figure 1. Graphical illustration of lignin and cross-linkers forming a recyclable loop system.

ability. The strength of a Si–O bond is comparable to a C–C bond, which affords its stability during usage.³⁰ However, the Si–O bond is highly susceptible to cleavage under various chemical conditions.^{31,32} Additionally, most silyl ether compounds are easy to make and cost-effective. Considering all these attributes, herein, we combine thiol-ene click chemistry with silyl ether cross-linkers to make recyclable lignin thermosets, as illustrated in Figure 1.

EXPERIMENTAL SECTION

Materials. Organosolv lignin (Lignol Corporation, $M_{\rm n}=1200~{\rm g}~{\rm mol}^{-1}, D=4.4$, the hydroxyl value = 5.62 mmol g⁻¹), allyl bromide (99%, Alfa Aesar), sodium hydroxide (NaOH 99%, Fisher Scientific), 10-undecen-1-ol (98%, Sigma Aldrich), imidazole (99%, VWR), 2-mercaptoethanol (99%, Sigma Aldrich), 6-mercapto-1-hexanol (98%, TCI), benzoin (98%, TCI), thioacetic acid (97%, Alfa Aesar), dichlorodiisopropylsilane (98%, TCI), tetrachlorosilane (98%, TCI), methanol (MeOH), dichloromethane (DCM), tetrahydrofuran (THF), and all other reagents were from commercial resources and used as received.

Lignin Allylation. A procedure was modified according to the literature. ²² Unfractionated lignin (5.5 g) was dissolved in THF (60 mL) and stirred until the solution was homogenous with a light brown color. Sodium hydroxide (5.5 g, 137.5 mmol) was then dissolved in deionized water (4 mL) and added to the lignin solution. The resulting mixture was stirred while allyl bromide (6.5 g, 53.7 mmol) was slowly added, the temperature was set to 65 °C, and the reaction was allowed to stir for 48 h. Afterward, the reaction was quenched by adding 0.1 M HCl and the resulting precipitate was placed under a rotary evaporator to remove the solvent. The brown solid was washed with water and then dried under vacuum with a final dry weight of 7.13 g. The total conversion of hydroxyl groups to ally groups was calculated to be about 95% according to ³¹P NMR.

Cross-Linker Synthesis. For mercapto alcohols, 2-mercaptoethanol and 6-mercapto-1-hexanol are commercially available, 11mercapto-1-undecanol was synthesized as follows. 10-Undecen-1-ol (8 g, 47 mmol) was added to a dry flask with a stir bar. Thioacetic acid (3.6 g, 47 mmol) was added, and the mixture was purged with N₂ for 10 min. Benzoin (200 mg, 0.9 mmol) was then dissolved in methanol (0.25 mL) and added to the flask. The reaction was then exposed to UV light (355 nm) overnight, and the resulting mixture was washed with cold DCM and then recrystallized with cold methanol to afford crude S-(11-hydroxyundecyl) ethanethioate. The thioester was then refluxed in methanol with sodium hydroxide (4 equiv) for 12 h. The reaction was then neutralized with 2 M HCl in ice and mixed with 200 mL of diethyl ether. The organic layer was separated, washed with 100 mL of brine, dried over magnesium sulfate, and filtered. The filtrate was concentrated and then freezedried to afford 9.4 g of white powder to give 11-mercapto-1undecanol.

Six different cross-linkers were synthesized using three mercapto alcohols and two silanes, as described here. In a round bottom flask

equipped with a stir bar, a mercapto alcohol was added to dry DCM and stirred at 0 $^{\circ}$ C in an ice bath. Imidazole (1 equiv) was added, and the reaction was purged with nitrogen for 10 min. Then, a silane (0.25 equiv for tetrachlorosilane and 0.5 equiv for dichlorodiisopropylsilane) was added dropwise and a white precipitate formed immediately. The reaction was allowed to warm to room temperature and react overnight. The solvent was then evaporated, and the remaining white precipitate was washed with ether. The ether solution was then dried leaving a yellow liquid. Purification by column chromatography on silica gel (15:1 hexane/ethyl acetate) provided a clear foul-smelling liquid.

Thiol-Ene Thermoset Formation. Various feed ratios of allyl lignin and di/tetra thiols were used. Here, LT-29 is used as a representative example (refer to Table 2). In a 10 mL dram vial, 200 mg of allylated lignin was added along with 200 mg of DSE-11. A total of 2 mL of THF was added, and the solution was sonicated and stirred for 1 min. After the solution became homogenous, it was poured into a Teflon mold. The THF was allowed to evaporate overnight, and the mold was then put into a vacuum oven at 120 °C and cured for 1 day and then put under vacuum for another day before testing.

Thermoset Deconstruction and Reconstruction. Using LT-29 as an example, 3.2 g of LT-29 (see Table 2) was placed in a round bottom flask along with a stir bar. A total of 2.6 g of tetrabutylammonium fluoride was dissolved in 10 mL of THF to form a 1 M solution and added to the flask. Alternatively, a 0.1 M solution of NaOH (aq.) was added at 40 °C overnight. The reaction was stirred overnight, and the resulting mixture was precipitated in water three times. The precipitant was dissolved in THF, filtered, and concentrated to a dark brownish-colored viscous liquid that was then dried under vacuum to a dark brown solid. The recovered solid mass after deconstruction was weighed at 3.1 g, which only had a loss of mass less than 5%. The materials were reconstructed using the aforementioned lignin allylation process, after which the mass increased to 3.8 g. Based on the initial allylation of lignin, the yield of mass increase was calculated to be about 94%.

■ CHARACTERIZATION

Fourier Transform Infrared Spectroscopy (FT-IR). FT-IR spectra of samples were recorded on a PerkinElmer spectrum 100 FTIR spectrometer using an attenuated total reflection (ATR) method. Absorption spectra were recorded at 4 cm⁻¹ resolution, and the signal averaged over 32 scans.

Gel Permeation Chromatography (GPC). The molecular weight $(M_{\rm n})$ and dispersity (\mathcal{D}) of polymers were determined and conducted on a Varian 390-LC system. A refractive index detector and 3 × PLgel 10 μ m mixed-BLS columns (300 × 7.5 mm) were employed using THF as an eluent at 30 °C. The flow rate of THF is set at 1.0 mL min⁻¹. The GPC system was calibrated with polystyrene (PS) from PSS Laboratories.

Nuclear Magnetic Resonance Spectroscopy (NMR). NMR spectra were recorded on a Bruker Avance III (400 or 300 MHz). Chemical shifts are reported in ppm with TMS as an internal standard (TMS 0.00 ppm for ^1H and ^{13}C or DMSO δ 2.5 ppm and 39.52 for ^1H and ^{13}C , respectively). For ^{31}P NMR experiments, 2—chloro-4,4,5,5-tetramethyl-1,3,2-dioxaphospholane was used to quantify the hydroxyl groups, and N-hydroxy-5-norbornene-2,3-dicarboximide was used as an internal standard following a previously published procedures. 33,34

Thermogravimetric Analysis (TGA). Thermogravimetric analysis (Hitachi 7200) was used to analyze the thermal properties of thermosets. A sample (10–15 mg) was encapsulated in a 60 μ L Pt pan. The sample was then heated to 800 °C with a heating rate of 10 °C/min under a nitrogen atmosphere.

Differential Scanning Calorimetry (DSC). A differential scanning calorimeter (Hitachi 7020) was used to analyze the thermal properties of thermosets. A sample (5–10 mg) was encapsulated in a 40 μ L aluminum pan. The sample was submitted (I) heating from 25 to 150 °C, (II) cooling to -60 °C, and (III) heating to 150 °C with cooling and heating rates at 10 °C/min under a nitrogen atmosphere.

Inductively Coupled Plasma Mass Spectrometry (ICP-MS). The samples were digested with 4 mL of aqua regia at 180 °C for 5 h, and the digestates were brought to 5 mL and analyzed using a Finnigan ELEMENT XR double focusing magnetic sector field inductively coupled plasma-mass spectrometer (SF-ICP-MS). A 0.2 mL/min Micromist Useries nebulizer (GE, Australia), quartz torch, and injector (Thermo Fisher Scientific, USA) were used for sample introduction.

Tensile Testing. Tensile stress—strain testing was conducted on an Instron 5543A testing instrument. Thermoset samples were prepared using a PTFE dog-bone mold with a cross-sectional length of 20 mm and a width of 5.0 mm. The thickness was between 0.29 and 0.31 mm. After evaporation of the solvent, the materials were dried under vacuum for 12 h at room temperature. Tests were done at room temperature with a crosshead speed of 1 mm min⁻¹.

RESULTS AND DISCUSSION

Modification of Lignin and Synthesis of Cross-Linkers. Unfractionated Organosolv lignin was used, which has molar mass around 1200 g/mol with a dispersity of $D \approx 4.4$. Lignin was allylated by reacting allyl bromide with alcohols in lignin under alkaline conditions. The conversion was measured quantitatively using ³¹P NMR, following a previously established procedure, ³⁴ in which 2—chloro-4,4,5,5-tetramethyl-1,3,2-dioxaphospholane was used to react with all hydroxyl groups and N-hydroxy-5-norbornene-2,3-dicarboximide was used as an internal standard. ³¹P NMR revealed a hydroxyl content of 5.6 mmol OH g⁻¹ for the virgin lignin (Table 1). ³³ After the lignin was allylated, the same analysis was used to

Table 1. ³¹P NMR Quantification of Hydroxyl Groups and Carboxylic Acid in Lignin

lignin	aliphatic alcohol (mmol/g)	phenolic alcohol (mmol/g)	carboxylic acid (mmol/g)
organosolv	1.1	4.2	0.3
allylated	0.1	~ 0.0	0.1

determine the remaining hydroxyl group content, which can determine the total conversion from hydroxyl groups to allyl groups at 96%. Unsurprisingly, virtually all the phenolic alcohol groups were reacted, while over 90% aliphatic alcohols were consumed (Figure 2). ¹H NMR and IR spectra (Figures S1 and S2) further supported this transformation with the presence of allyl groups. NMR characterization shows that the phenolic and aliphatic hydroxyl groups were converted to the allyl ethers. The alkenylation is also evident by the increase in solubility of modified lignin in THF, acetone, and ethyl acetate compared to the virgin samples.

The cross-linkers are designed to possess a few functionalities. First, they can promote thermal thiol-ene "click" chemistry to react with allylated lignin. Second, the cross-linkers possess tunable cross-linking densities. Third, they can enable a specific degradation pathway. Therefore, we combined silyl ether with thiol in difunctional and tetrafunctional structures. As shown in Scheme 1, silyl chlorides (dichloro and tetrachloro) were reacted with hydroxyl-capped thiols to create thiol-capped silyl ethers that could readily undergo thermal click reactions with allyl groups. Another aspect investigated was the length of spacers in cross-linkers. The hydroxyl-capped thiols were chosen with a spacer of 2, 6, and 11 methylenes. The library of cross-linkers is shown in Scheme 1.

To ensure that the silyl ethers could be chemically degraded, in a model reaction TBAF was added to a solution of cross-linker using DSE-6. The reaction was tracked via ¹H, ¹³C, and ¹H–²⁹Si HMBC NMR (Figures S3–S5). Disappearance of the alpha protons to the silyl ether confirms its degradation while the correlation between the Si and the methine proton in isopropyl remains intact. This indicated that only the Si–O bonds were cleaved.³⁵

Preparation and Characterization of Thermosets. Thermosets were synthesized using various lignin contents and different ratios of DSE:TSE. In comparison with lignin, allyl lignin has an enhanced solubility that facilitates the mixing with cross-linkers. Since the thiol-ene reaction proceeded via thermal initiation, the thermosets could be used directly for testing after curing. The incorporation of silyl ether cross-linkers into the thermosets was qualitatively measured using FTIR and solid state ¹³C and ²⁹Si NMR (Figure 3 and Figure S6) and ICP-MS (Table S1).

As shown in Figure 3b, FTIR spectra verify the presence of the cross-linkers with the appearance of stretching C–H and Si–O peaks at 2800 and 1100 cm⁻¹, respectively. Solid-state NMR spectra show the appearance of new chemical shifts at δ = 20–40 ppm, corresponding to the aliphatic carbons from the cross-linkers (Figure 3a). Furthermore, the decrease in peak intensity for the δ = 100–140 ppm and the formation of a new chemical shift around δ = 60 ppm indicate the conversion of alkenes to thioethers via the thiol-ene reaction. Further studies using ²⁹Si NMR confirmed the presence of Si in the material at δ = 100 ppm, which corresponds to the chemical shift of the cross-linker (Figure S6).

The mechanical properties were then examined using tensile testing (Table 2). Initially, dithiolsilyl ether (DSE-2) was used as a difunctional cross-linker to evaluate the curing processing with different weight fractions of lignin (Figure 4a). With the weight fraction of lignin at 33 wt %, the thermoset was too soft to be measured by the tensile testing. Increasing the lignin content to 50% and then to 66% greatly increases the tensile strength of the thermosets to 0.19 and 0.63 MPa, respectively.

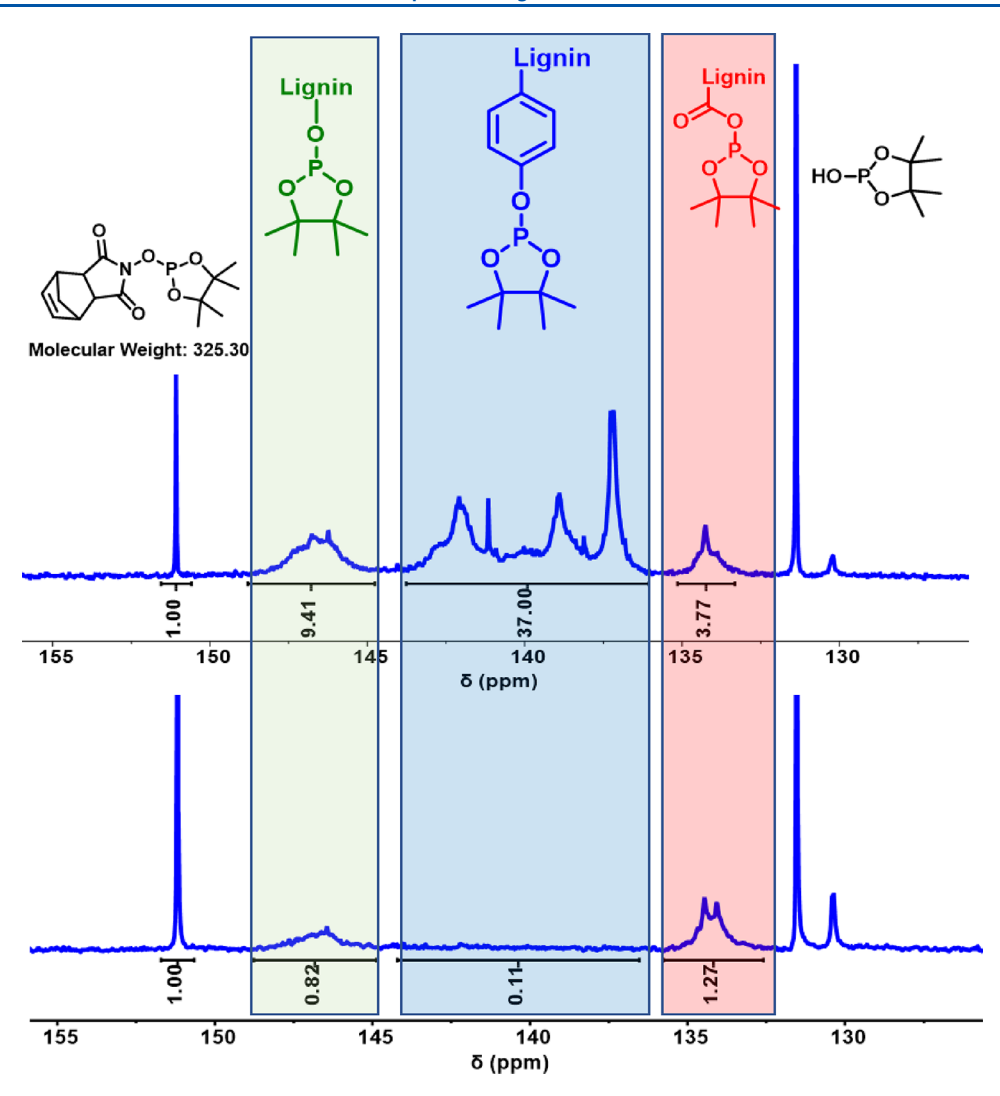


Figure 2. ³¹P NMR spectral analysis of different hydroxyl and carboxylic acid groups: (top) Organosolv lignin; (bottom) allylated lignin.

We then evaluated the effect of spacers in difunctional crosslinkers on the mechanical properties. Figure 4b,c shows the tensile profiles using DSE-6 and DSE-11. When the crosslinker was maintained the same, the tensile strength increases with the increase of lignin content. However, when the lignin content was maintained constant, cross-linkers with a longer spacer resulted in high tensile strength. With 66 wt % lignin, the use of DSE-11 led to the thermosets with the tensile strength of 2.10 MPa. This observation was initially counterintuitive, as one would expect the longer spacer to reduce the cross-linking density and thus weaken the thermoset. However, it may be related to the efficiency of cross-linkers affected by the length of a spacer. When the spacer is very short (e.g., DSE-2), the inflexibility of the spacer could significantly reduce the cross-linking efficiency. By contrast, the flexibility of the long spacer could raise the cross-linking efficiency. By contrast, the flexibility of the long spacer could raise the cross-linking efficiency, as illustrated in Figure 5a. This explanation was supported by FTIR spectra, which show that the thiol groups were present in thermosets using DSE-2 but not the one using DSE-11 (Figure 5b).

The scenario in the case of a tetrafunctional cross-linker is quite different. It is expected that TSE could lead to efficient cross-linking, regardless the length of spacers. Thus, the

presence of a shorter spacer with less flexibility would lead to more brittle thermosets. This was exactly what was observed. With the use of either TSE-2 or TSE-6 as a cross-linker, all thermosets are very brittle. The only thermoset, which can form a free-standing film, is the one when TSE-11 that carries flexible long spacers was used with only 33 wt % lignin (Figure 4d). This thermoset, compared to the one containing DSE-11 with 33 wt % lignin, has a much smaller tensile strain (~4% vs ~45%) yet a much higher tensile strength (~1.75 MPa vs ~0.5 MPa). The changes in the stress—strain curve are consistent with the increase of cross-linking density when TSE-11 replaces DSE-11.

The above mechanical characterization demonstrated that incorporating either too much lignin or TSE led to very brittle thermosets. We then investigated the effect of a mixture of DSE and TSE on the mechanical properties of thermosets. DSE and TSE were combined in molar ratios of 1.0:0.5, 1.0:1.0, and 1.0:2.0. These ratios were chosen to examine which cross-linker has a more profound effect on mechanical strength. DSE-11/TSE-11 showed the highest strength among the materials tested and are presented in Figure 6.

We first evaluated the mixtures of DSE-6 and TSE-6 and compared them with the one only using DSE-6. With the lignin at 50 wt % (Figure 6a), the incorporation of TSE-6

Scheme 1. Synthesis and Click Chemistry of Allyl Lignin and Thiol Silyl Ethers and Library of Cross-Linkers. (a) Synthesis of Allyl Lignin; (b) Synthesis of Thiol Silyl Ethers (DSE-X or TSE-X, Where D and T Refer to Dithiol and Tetrathiol, Respectively, and X Is the Number of Carbons between Sulfur and Oxygen); (c) Click Chemistry between Allyl Lignin and Thiol Silyl Ethers; (d) A Library of Thiol Silyl Ethers as Cross-Linkers

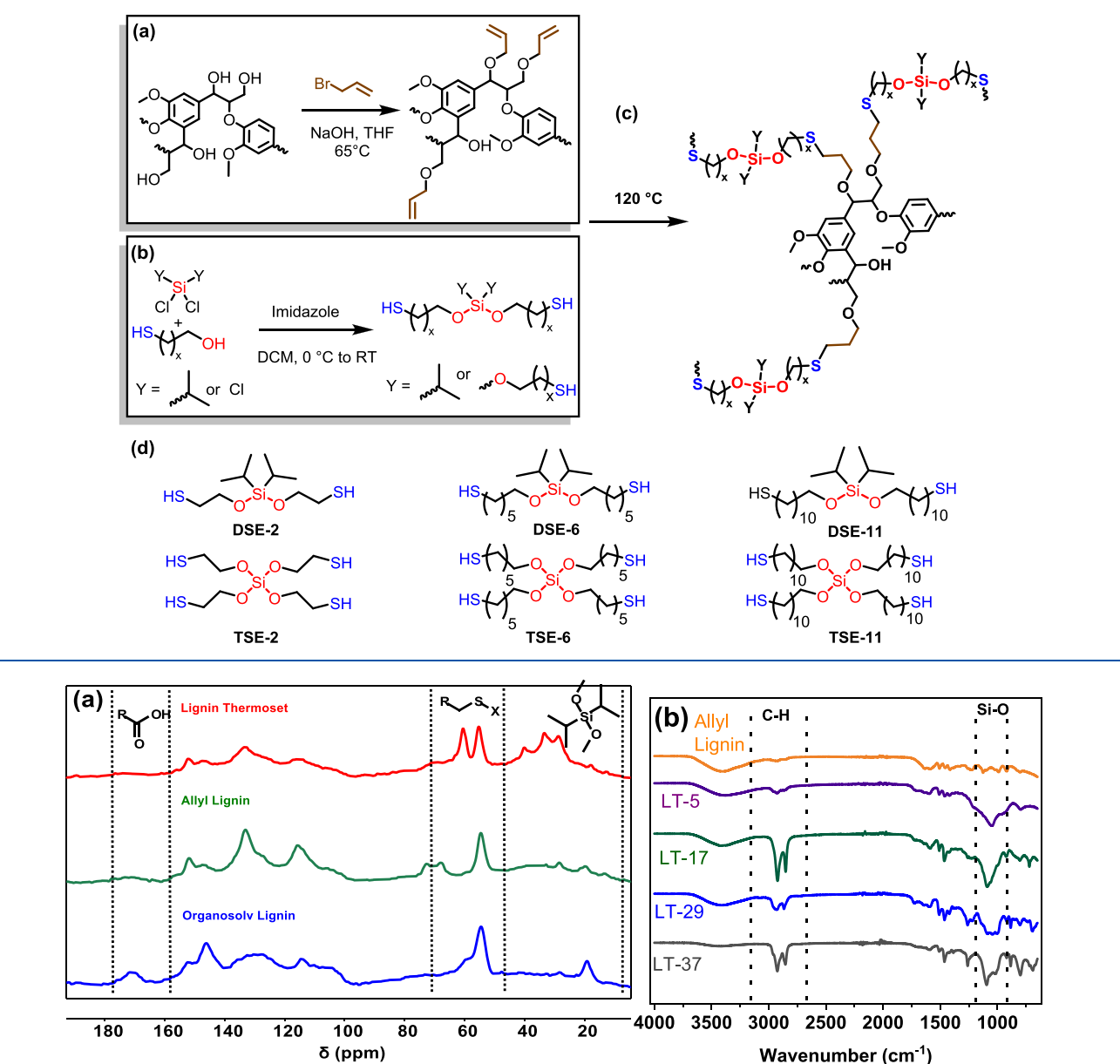


Figure 3. (a) CP-MAS ¹³C NMR spectra of organosolv lignin (blue), allyl lignin (green), and lignin thermoset (red); (b) FTIR spectra of lignin thermosets using different cross-linkers.

substantially increased the stress while having a small reduction of tensile strain. With the increase of lignin fraction to 66 wt % (Figure 6b), the mixtures of cross-linkers resulted in thermosets much stronger than those with 50 wt % lignin and also the thermoset using only DSE-6 with the same amount of lignin. These results were not surprising, as it was expected that either increasing the fraction of lignin or incorporating more TSE cross-linker would lead to higher stress and lower tensile strain. However, when the cross-linkers with a longer spacer (DSE-11 and TSE-11) were mixed, the results are significantly different. With the fraction of lignin at 50 wt % (Figure 6c), all mixtures of cross-linkers led to lower strain at break (from 33 to 15%) compared to the use of only

DSE, while maintaining similar levels of stress at break (~0.65 MPa). This result on stress was quite surprising. Perhaps under this level of lignin, the cross-linking reactions involving TSE may not be highly efficient, leaving some of thiol groups dangling. The impact on stress from the increase of cross-linking density would be offset by the dangling groups. When the lignin fraction increased to 66 wt % (Figure 6d), an appreciable increase of cross-linking density resulted in higher stress at break (by 0.25 to 0.5 MPa) and much smaller strain at break (~10% or smaller). Since a higher fraction of lignin has more ally groups, it would consume more cross-linkers that were incorporated into the thermosets, enhancing the cross-linking density, thus leading to higher stress and lower strain.

Table 2. Selected Lignin Thermosets: Compositions and Mechanical Properties^a

sample code	lignin (wt %)	cross-linker spacer length	DSE:TSE (molar ratio)	tensile strength (MPa)	tensile strain (%)
LT-5	50	2	1.0:0.0	0.19	24.3
LT-6			1.0:0.5	0.21	20.1
LT-7			1.0:1.0	0.24	19.7
LT-8			1.0:2.0	0.26	19.6
LT-9	66	2	1.0:0.0	1.00	21.9
LT-10			1.0:0.5	1.20	6.9
LT-11			1.0:1.0	1.20	7.8
LT-12			1.0:2.0	1.30	6.4
LT-17	50	6	1.0:0.0	0.33	20.2
LT-18			1.0:0.5	0.54	16.3
LT-19			1.0:1.0	0.40	14.3
LT-20			1.0:2.0	0.46	15.9
LT-21	66	6	1.0:0.0	1.43	10.7
LT-22			1.0:0.5	1.60	4.4
LT-23			1.0:1.0	1.80	5.9
LT-24			1.0:2.0	1.50	6.1
LT-29	50	11	1.0:0.0	0.66	29.5
LT-30			1.0:0.5	0.68	17.7
LT-31			1.0:1.0	0.67	14.6
LT-32			1.0:2.0	0.67	26.0
LT-33	66	11	1.0:0.0	2.10	28.7
LT-34			1.0:0.5	2.30	4.9
LT-35			1.0:1.0	2.70	7.1
LT-36			1.0:2.0	2.60	10.8
LT-37	33	11	0.0:1.0	1.70	3.0
a-1 1					

^aThe lignin wt % refers to the feed weight fraction.

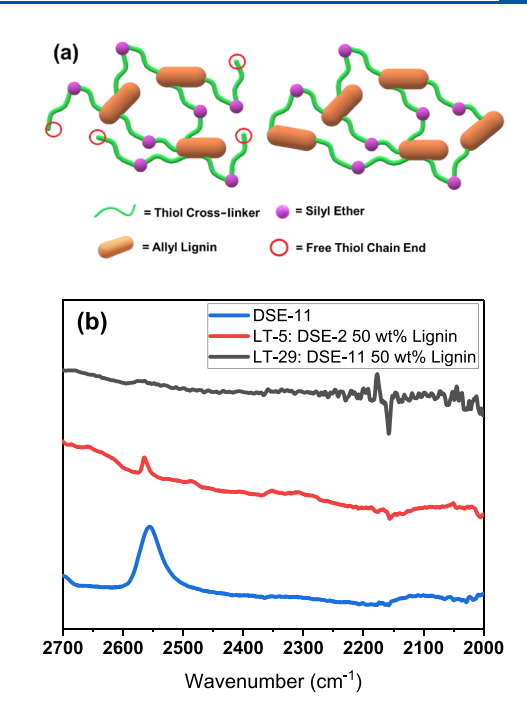


Figure 5. (a) Graphical representation of short DSE-2 cross-linker vs long DSE-11 cross-linker; (b) FTIR spectra of thermosets using DSE-11, DSE-2, or DSE 11 at 50 wt % lignin.

Deconstruction and Reconstruction of Thermosets.

We then carried out the deconstruction of thermosets and evaluated the plausibility of reconstruction using thermoset LT-29 with DSE-11 as a cross-linker (Figure 7). Silyl ethers are known to degrade readily when reacted with fluoride. 35,32

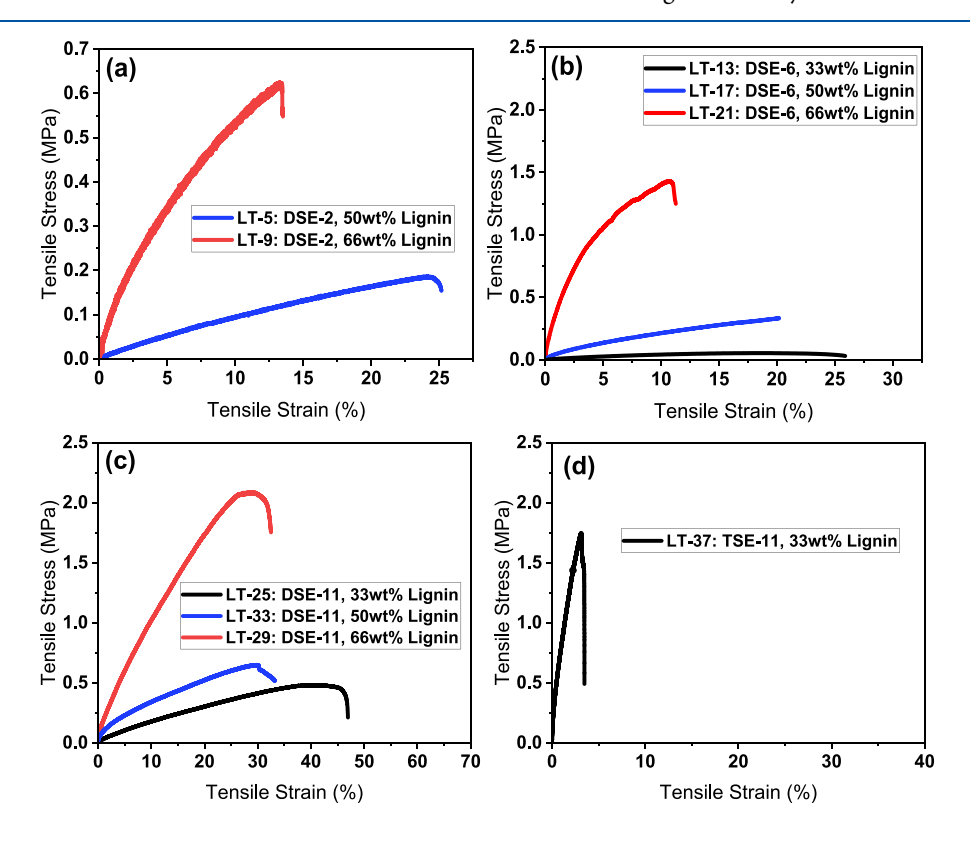


Figure 4. (a) Tensile curves of thermosets using DSE-2 (50 and 66 wt % lignin); (b) tensile curves of thermosets using DSE-6 (33, 50, and 66 wt % lignin); (c) tensile curves of thermosets using DSE-11 (33, 50, and 66 wt % lignin); (d) tensile curve of thermosets using TSE-11 (33 wt % lignin).

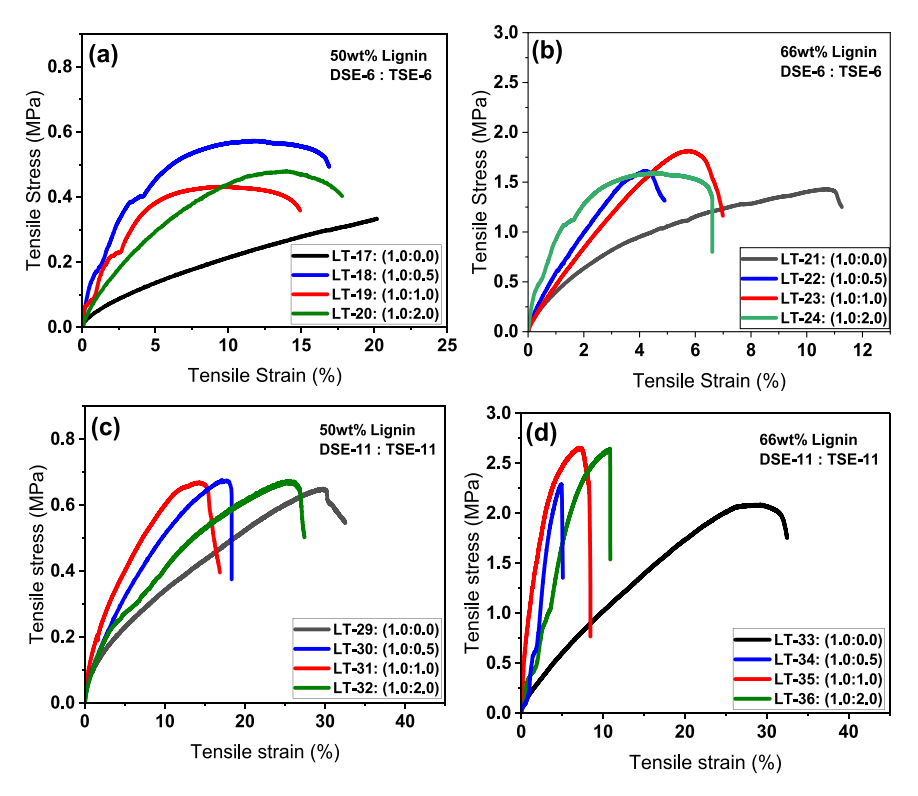


Figure 6. Tensile curves of thermosets using a mixture of DSE-6:TSE-6: (a) 50 wt % lignin; (b) 66 wt % lignin; tensile curves of thermosets using a mixture of DSE-11:TSE-11: (c) 50 wt % lignin; (d) 66 wt % lignin.

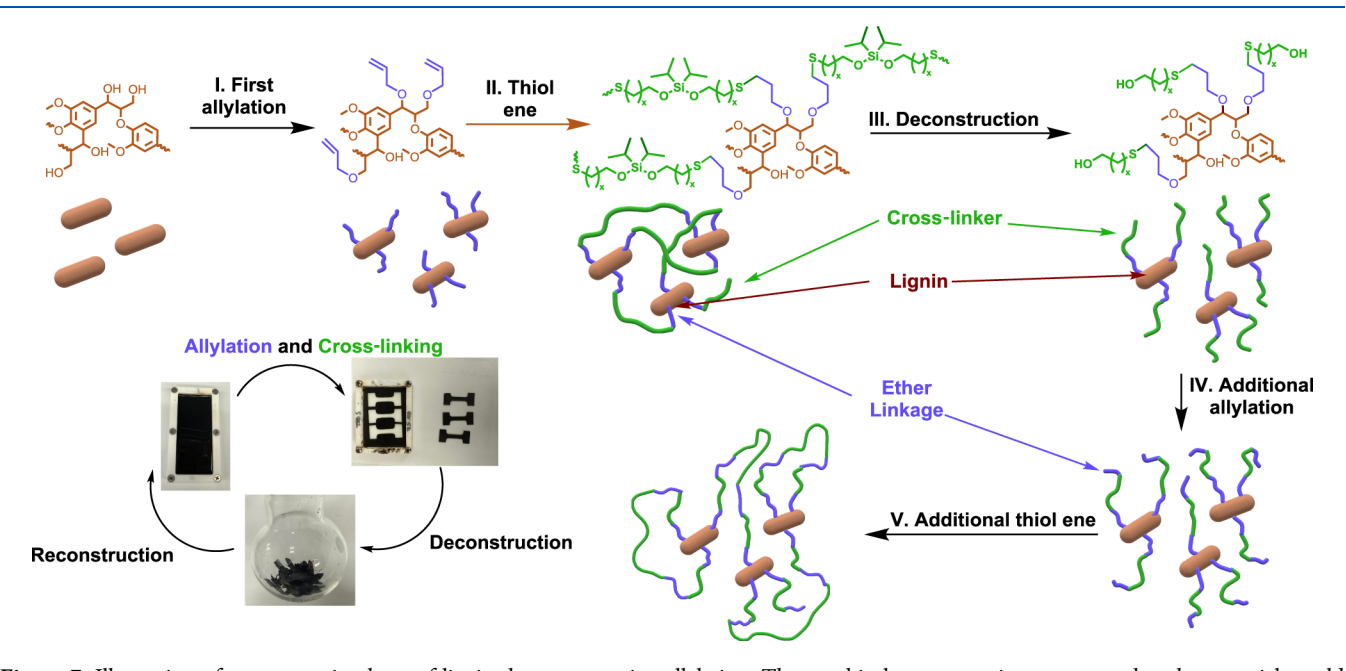


Figure 7. Illustration of a reprocessing loop of lignin thermosets using allylation. The graphical representation suggests what the material would look like after one cycle of reconstruction. Optical images are included for reference.

However, fluoride poses safety concerns; thus, 0.1 M sodium hydroxide in a mixture of water and THF was explored in this work to evaluate possible degradation mechanisms for these thermosets. It was also found that degradation under the basic condition occurred rapidly regardless of the weight fraction of lignin in the thermosets, as the initial heterogeneous mixtures became homogeneous solutions (Figure S7). Both solutions were then subject to filtration to remove any remaining cross-linked materials. As described in the Experimental Section, we

determined the mass recovery of both lignin deconstruction and reconstruction of lignin allylation. The first step was observed with less than 5 wt % loss, which corresponded to the very small fraction of disopropyl silicone. The re-allylation step had a high yield at 94%, which was similar to the initial allylation. The deconstruction process was supported by FTIR studies. The appearance of a broad peak around 3200 cm⁻¹ indicated the presence of hydroxyl and C–H stretching (Figure 8).

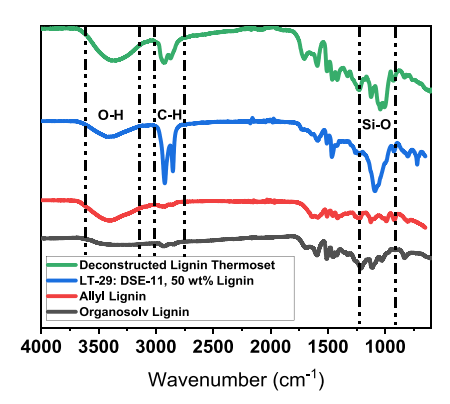


Figure 8. FTIR spectra of organosolv lignin, allyl lignin, thermoset LT-29, and deconstructed thermoset.

In parallel, we also evaluated the deconstruction using NMR characterization. However, to improve the signal accuracy, we chose LT-5 (with DSE-2 as a cross-linker) because it is more convenient for NMR analysis due to the fewer methylene groups in the spacer of the cross-linker. Reappearance of the O–H and C–H suggests that the alkyl spacer chain remained on lignin and the Si–O–C bonds were converted to hydroxyl groups on lignin (Figure 9b). Furthermore, any esters formed from the allylation of carboxylic acid would convert to the

corresponding acid under basic conditions followed by aqueous workup. However, since the degradation using TBAF produced similar results it is unlikely that the acid moieties contribute to the -OH signal in IR. 2D NMR was used to understand the deconstruction mechanism (Figure 9). Lignin allylation resulted in two new shifts around δ 5.5 ppm corresponding to two unique carbons around δ 130 ppm, which is characteristic of terminal alkenes and in line with previously reported modifications (Figure 9b).³⁷ The deconstructed structures of thermosets observed the disappearance of the allyl signals around δ 5.5 ppm in ${}^{1}H$ spectrum and the appearance of alpha thioether signals at δ 35 ppm in 13 C spectrum (Figure 9c). Furthermore, ¹H NMR shows the appearance of a broad peak at δ 2.5 ppm, which has similar chemical shifts to the alkyl chain of the cross-linker (Figure 9d), suggesting that the spacer chain, alkyl group from the cross-linker, was maintained on the lignin surface (Figure S4).

Reconstructing the degraded thermosets was then explored. The first route was the direct silylation on the deconstructed lignin thermosets. This route presented several disadvantages. First, the addition of imidazole to catalyze the reaction made workup harder when trying to remove the catalyst. Second, the sensitivity of silyl chlorides to moisture made measuring precise amounts difficult unless inert air-free environments were employed. Finally, the byproducts of the silyl ether formation weakened the final material. HCl gas from the

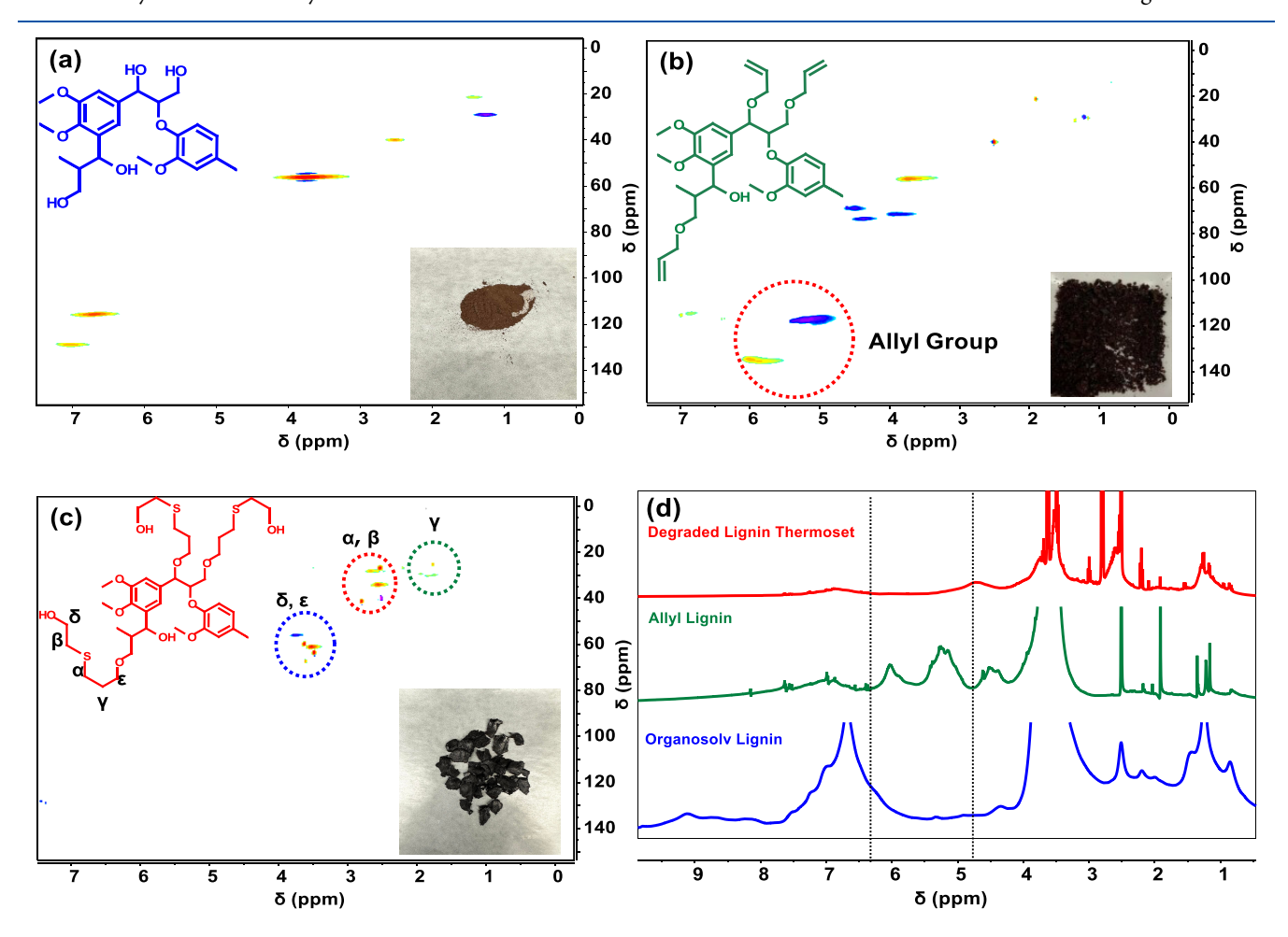
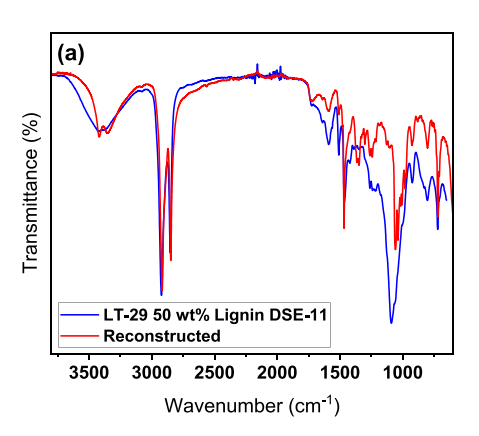


Figure 9. 13 C- 1 H HSQC NMR spectra: (a) organosolv lignin; (b) allyl lignin; (c) deconstructed lignin thermoset (from LT-5); (d) 1 H NMR spectra of organosolv lignin, allylated lignin, and deconstructed lignin thermoset. Insets in (a-c) are optical images of respective lignin samples. LT-5 was chosen because it is more convenient for NMR analysis due to the few methylene groups in the spacer.



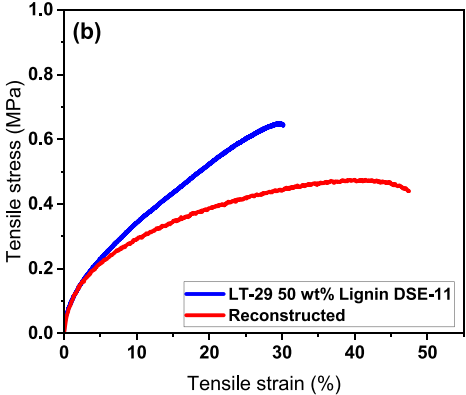


Figure 10. (a) FTIR spectra and (b) tensile curves of LT-29 for the initial and reconstructed thermosets.

reaction creates bubbles in the reformed material that adds weak points under stress. The silyl chloride may also undergo polymerization with water to form polysiloxanes, which would introduce heterogeneity into the thermosets. These drawbacks encouraged us to pursue a more facile route to thermoset reconstruction.

The deconstructed thermosets were reacted with allyl bromide followed by thiol-ene click chemistry with the cross-linker DSE-2. The entire process employed the same route as used for the virgin Organosolv lignin initially (Figure 7). The major byproducts formed are sodium salts, which can be easily removed with an aqueous wash. This route possesses several advantages. No side products were formed that could require tedious purification or cause heterogeneity in the thermosets.⁴⁰

An additional DSE-11 cross-linker was used to reconstruct degraded LT-29 after allylation to create a free-standing film. The reconstructed LT-29 was compared to the original thermoset using FTIR and found to have very similar absorptions, indicating there were minimal, unintended transformations (Figure 10a) Next, the mechanical properties were studied using tensile testing and were found to differ from the original thermoset (Figure 10b). A reduction in tensile stress was observed from 0.65 to 0.46 MPa, and an increase in strain at break from 30% to 43% occurred. After the deconstruction, there are additional spacers between periphery hydroxyl groups and the lignin core. The addition of the crosslinker in the reconstruction process would further extend the linear chains, thioethers, and ethers of between lignin cores. Thus, it would not be a surprise to observe the change of mechanical properties. Similar systems have been reported a decrease in stress and an increase in stretchability with ethylene glycol cross-linkers.⁴¹

CONCLUSIONS

We developed a facile approach to the preparation of lignin thermosets via thiol-ene click chemistry. Several thiol ether cross-linkers were synthesized and incorporated into a fully sustainable thermoset composed of lignin using thermal curing. The mechanical properties of the thermosets were measured and strongly correlated with the structures and density of cross-linkers as well as the fraction of lignin in the thermosets. Deconstruction experiments were performed on of these thermosets, which were degradable under alkaline conditions. The reconstruction process enabled the reformation of thermosets.

ASSOCIATED CONTENT

Supporting Information

The Supporting Information is available free of charge at https://pubs.acs.org/doi/10.1021/acs.macromol.2c02428.

³¹P NMR spectra, ¹H NMR spectra, and FTIR spectra of different lignin materials; ¹H NMR, ¹³C NMR, and ²⁹Si-¹H HSQC spectra for synthesized cross-linkers and model degradation; and ICP data, FTIR, and optical photos for different lignin thermosets (PDF)

AUTHOR INFORMATION

Corresponding Authors

Ting Ge — Department of Chemistry and Biochemistry, University of South Carolina, Columbia, South Carolina 29208, United States; ⊚ orcid.org/0000-0003-2456-732X; Email: tingg@mailbox.sc.edu

Chuanbing Tang — Department of Chemistry and Biochemistry, University of South Carolina, Columbia, South Carolina 29208, United States; orcid.org/0000-0002-0242-8241; Email: tang4@mailbox.sc.edu

Authors

Yishayah Bension — Department of Chemistry and Biochemistry, University of South Carolina, Columbia, South Carolina 29208, United States

Leman Buzoglu Kurnaz – Department of Chemistry and Biochemistry, University of South Carolina, Columbia, South Carolina 29208, United States

Complete contact information is available at: https://pubs.acs.org/10.1021/acs.macromol.2c02428

Notes

The authors declare no competing financial interest.

■ ACKNOWLEDGMENTS

The authors would like to acknowledge the support from the U.S. National Science Foundation (DMR1806792). T.G. acknowledges start-up funding from the University of South Carolina. This work was supported in part by the National Science Foundation EPSCoR Program under NSF grant no. OIA-1655740.

REFERENCES

(1) Cook, W. D.; Mayr, A. E.; Edward, G. H. Yielding behaviour in model epoxy thermosets — II. Temperature dependence. *Polymer* **1998**, *39*, *3725–3733*.

- (2) Vidil, T.; Tournilhac, F.; Musso, S.; Robisson, A.; Leibler, L. Control of reactions and network structures of epoxy thermosets. *Prog. Polym. Sci.* **2016**, *62*, 126–179.
- (3) Farshchi, N.; Gedan-Smolka, M. Polyurethane Powder Coatings: A Review of Composition and Characterization. *Ind. Eng. Chem. Res.* **2020**, *59*, 15121–15132.
- (4) Geyer, R.; Jambeck, J. R.; Law, K. L. Production, use, and fate of all plastics ever made. *Sci. Adv.* **2017**, *3*, No. e1700782.
- (5) Wang, Z.; Ganewatta, M. S.; Tang, C. Sustainable polymers from biomass: Bridging chemistry with materials and processing. *Prog. Polym. Sci.* **2020**, *101*, 101197.
- (6) Wang, Z.; Yuan, L.; Tang, C. Sustainable Elastomers from Renewable Biomass. Acc. Chem. Res. 2017, 50, 1762–1773.
- (7) Liu, Y.; Yu, Z.; Wang, B.; Li, P.; Zhu, J.; Ma, S. Closed-loop chemical recycling of thermosetting polymers and their applications: a review. *Green Chem.* **2022**, *24*, 5691–5708.
- (8) Pérez, R. L.; Ayala, C. E.; Opiri, M. M.; Ezzir, A.; Li, G.; Warner, I. M. Recycling Thermoset Epoxy Resin Using Alkyl-Methyl-Imidazolium Ionic Liquids as Green Solvents. *ACS Appl. Polym. Mater.* **2021**, *3*, 5588–5595.
- (9) Ma, S.; Webster, D. C. Degradable thermosets based on labile bonds or linkages: A review. *Prog. Polym. Sci.* **2018**, *76*, 65–110.
- (10) Kloxin, C. J.; Scott, T. F.; Adzima, B. J.; Bowman, C. N. Covalent Adaptable Networks (CANs): A Unique Paradigm in Cross-Linked Polymers. *Macromolecules* **2010**, *43*, 2643–2653.
- (11) Zhao, X.-L.; Tian, P.-X.; Li, Y.-D.; Zeng, J.-B. Biobased covalent adaptable networks: towards better sustainability of thermosets. *Green Chem.* **2022**, 24, 4363–4387.
- (12) Mahajan, J. S.; O'Dea, R. M.; Norris, J. B.; Korley, L. T. J.; Epps, T. H., III Aromatics from Lignocellulosic Biomass: A Platform for High-Performance Thermosets. *ACS Sustainable Chem. Eng.* **2020**, *8*, 15072–15096.
- (13) Coates, G. W.; Getzler, Y. D. Y. L. Chemical recycling to monomer for an ideal, circular polymer economy. *Nat. Rev. Mater.* **2020**, *5*, 501–516.
- (14) Ganewatta, M. S.; Wang, Z.; Tang, C. Chemical syntheses of bioinspired and biomimetic polymers toward biobased materials. *Nat. Rev. Chem.* **2021**, *5*, 753–772.
- (15) Korley, L. T. J.; Epps, T. H., III; Helms, B. A.; Ryan, A. J. Toward polymer upcycling—adding value and tackling circularity. *Science* **2021**, *373*, 66–69.
- (16) Feofilova, E. P.; Mysyakina, I. S. Lignin: Chemical structure, biodegradation, and practical application (a review). *Appl. Biochem. Microbiol.* **2016**, *52*, 573–581.
- (17) Ganewatta, M. S.; Lokupitiya, H. N.; Tang, C. Lignin Biopolymers in the Age of Controlled Polymerization. *Polymer* **2019**, *11*, 1176.
- (18) Chung, H.; Washburn, N. R. Chemistry of lignin-based materials. *Green Mater.* **2013**, *1*, 137–160.
- (19) Bajwa, D. S.; Pourhashem, G.; Ullah, A. H.; Bajwa, S. G. A concise review of current lignin production, applications, products and their environmental impact. *Ind. Crops Prod.* **2019**, *139*, 111526.
- (20) Zhou, X. C.; Sjöberg, R.; Druet, A.; Schwenk, J. M.; van der Wijngaart, W.; Haraldsson, T.; Carlborg, C. F. Thiol-ene-epoxy thermoset for low-temperature bonding to biofunctionalized microarray surfaces. *Lab Chip* **2017**, *17*, 3672–3681.
- (21) Li, C.; Johansson, M.; Sablong, R. J.; Koning, C. E. High performance thiol-ene thermosets based on fully bio-based poly-(limonene carbonate)s. *Eur. Polym. J.* **2017**, *96*, 337–349.
- (22) Jawerth, M.; Johansson, M.; Lundmark, S.; Gioia, C.; Lawoko, M. Renewable Thiol–Ene Thermosets Based on Refined and Selectively Allylated Industrial Lignin. *ACS Sustainable Chem. Eng.* **2017**, *5*, 10918–10925.
- (23) Ribca, I.; Jawerth, M. E.; Brett, C. J.; Lawoko, M.; Schwartzkopf, M.; Chumakov, A.; Roth, S. V.; Johansson, M. Exploring the Effects of Different Cross-Linkers on Lignin-Based Thermoset Properties and Morphologies. *ACS Sustainable Chem. Eng.* **2021**, *9*, 1692–1702.

- (24) Xu, Y.; Yuan, L.; Wang, Z.; Wilbon, P. A.; Wang, C.; Chu, F.; Tang, C. Lignin and soy oil-derived polymeric biocomposites by "grafting from" RAFT polymerization. *Green Chem.* **2016**, *18*, 4974–4981.
- (25) Hwang, J.; Martinez, D. V.; Martinez, E. J.; Metavarayuth, G.; Goodlett, D.; Wang, Q.; Ganewatta, M.; Kent, M. S.; Tang, C. Highly swellable hydrogels prepared from extensively oxidized lignin. *Giant* **2022**, *10*, 100106.
- (26) Han, Y.; Yuan, L.; Li, G.; Huang, L.; Qin, T.; Chu, F.; Tang, C. Renewable polymers from lignin via copper-free thermal click chemistry. *Polymer* **2016**, *83*, 92–100.
- (27) Yuan, L.; Zhang, Y.; Wang, Z.; Han, Y.; Tang, C. Plant Oil and Lignin-Derived Elastomers via Thermal Azide–Alkyne Cycloaddition Click Chemistry. ACS Sustainable Chem. Eng. 2019, 7, 2593–2601.
- (28) Liu, H.; Mohsin, N.; Kim, S.; Chung, H. Lignin, a biomass crosslinker, in a shape memory polycaprolactone network. *J. Polym. Sci., Part A: Polym. Chem.* **2019**, *57*, 2121–2130.
- (29) Kurnaz, L. B.; Bension, Y.; Tang, C. Facile Catalyst-Free Approach toward Fully Biobased Reprocessable Lignin Thermosets. *Macromol. Chem. Phys.* **2023**, 224, 2200303.
- (30) Cottrell, T. L. The strengths of chemical bonds; Butterworths Scientific Publications: 1958.
- (31) Wuts, P. G. M.; Greene, T. W. Protection for the Hydroxyl Group, Including 1,2- and 1,3-Diols. In *Greene's Protective Groups in Organic Synthesis*; John Wiley & Sons: Hoboken, New Jersey, 2006; pp. 16–366.
- (32) Shieh, P.; Zhang, W.; Husted, K. E. L.; Kristufek, S. L.; Xiong, B.; Lundberg, D. J.; Lem, J.; Veysset, D.; Sun, Y.; Nelson, K. A.; Plata, D. L.; Johnson, J. A. Cleavable comonomers enable degradable, recyclable thermoset plastics. *Nature* **2020**, *583*, 542–547.
- (33) Meng, X.; Crestini, C.; Ben, H.; Hao, N.; Pu, Y.; Ragauskas, A. J.; Argyropoulos, D. S. Determination of hydroxyl groups in biorefinery resources via quantitative 31P NMR spectroscopy. *Nat. Protoc.* **2019**, *14*, 2627–2647.
- (34) Pu, Y.; Cao, S.; Ragauskas, A. J. Application of quantitative 31P NMR in biomass lignin and biofuel precursors characterization. *Energy Environ. Sci.* **2011**, *4*, 3154–3166.
- (35) DiLauro, A. M.; Seo, W.; Phillips, S. T. Use of Catalytic Fluoride under Neutral Conditions for Cleaving Silicon—Oxygen Bonds. *J. Org. Chem.* **2011**, *76*, 7352—7358.
- (36) Campos, L. M.; Killops, K. L.; Sakai, R.; Paulusse, J. M. J.; Damiron, D.; Drockenmuller, E.; Messmore, B. W.; Hawker, C. J. Development of Thermal and Photochemical Strategies for Thiol—Ene Click Polymer Functionalization. *Macromolecules* **2008**, *41*, 7063–7070.
- (37) Jawerth, M.; Lawoko, M.; Lundmark, S.; Perez-Berumen, C.; Johansson, M. Allylation of a lignin model phenol: a highly selective reaction under benign conditions towards a new thermoset resin platform. *RSC Adv.* **2016**, *6*, 96281–96288.
- (38) Rubinsztajn, S.; Cypryk, M.; Chojnowski, J. Condensation of model linear siloxane oligomers possessing silanol and silyl chloride end groups. The mechanism of silanol silylation by a chlorosilane in the presence of neutral nucleophiles. *J. Organomet. Chem.* **1989**, 367, 27–37.
- (39) Crouch, R. D. Recent advances in silyl protection of alcohols. *Synth. Commun.* **2013**, 43, 2265–2279.
- (40) Antoni, P.; Robb, M. J.; Campos, L.; Montanez, M.; Hult, A.; Malmström, E.; Malkoch, M.; Hawker, C. J. Pushing the Limits for Thiol–Ene and CuAAC Reactions: Synthesis of a 6th Generation Dendrimer in a Single Day. *Macromolecules* **2010**, *43*, 6625–6631.
- (41) Xu, Y.; Odelius, K.; Hakkarainen, M. One-Pot Synthesis of Lignin Thermosets Exhibiting Widely Tunable Mechanical Properties and Shape Memory Behavior. *ACS Sustainable Chem. Eng.* **2019**, 7, 13456–13463.